NASA Technical Memorandum 100562

AVSCOM Technical Memorandum 88-B-003

OPTIMAL PLACEMENT OF TUNING MASSES FOR VIBRATION REDUCTION IN HELICOPTER ROTOR BLADES

Jocelyn I. Pritchard and Howard M. Adelman

MARCH 1988

National Aeronautics and Space Administration

Langley Research Center
Hampton, Virginia 23665-5225

US ARMY AVIATION SYSTEMS COMMAND
AVIATION R&T ACTIVITY

OPTIMAL PLACEMENT OF TUNING MASSES FOR VIBRATION REDUCTION IN HELICOPTER ROTOR BLADES

Jocelyn I. Pritchard and Howard M. Adelman
NASA Langley Research Center
Hampton, Virginia

ABSTRACT

This paper describes methods for reducing vibration in helicopter rotor blades by determining the optimum sizes and locations of tuning masses through formal mathematical optimization techniques. An optimization procedure is developed which employs the tuning masses and corresponding locations as design variables which are systematically changed to achieve low values of shear without a large mass penalty. The finite-element structural analysis of the blade and the optimization formulation require the development of discretized expressions for two performance parameters: the modal shaping parameter and the modal shear amplitude. Matrix expressions for both quantities and their sensitivity derivatives are derived in this paper. Three optimization strategies are developed and tested. The first is based on minimizing the modal shaping parameter which indirectly reduces the modal shear amplitudes corresponding to each harmonic of airload. The second strategy reduces these amplitudes directly and the third strategy reduces the shear as a function of time during a revolution of the blade. The first strategy works well for reducing the shear for one mode responding to a single harmonic of the airload but has been found in some cases to be ineffective for more than one mode. The second and third strategies give similar results and show excellent reduction of the shear with a low mass penalty.

LIST OF SYMBOLS

A_k	Amplitude of the generalized force distribution
DAF_{ik}	Dynamic amplification factor
F_{ik}	Generalized force, lbf
$\{F_k\}$	Force vector, lbf
f, f_o	Objective function
g, g_o	Constraint function
I	Set of modes included in procedure
K	Set of harmonics of airload included in procedure
$[K]$	Elastic stiffness matrix, lbf/in
m	Mass per unit length, lbm/in
$[M]$	Mass matrix, lbm
$\bar{M}_i$	Generalized mass, lbm
M_n	Tuning mass, lbm
MSP	Modal shaping parameter
M_{TOT}	Total tuning mass, lbm
NCON	Number of constraints
NDV	Number of design variables
NHARM	Number of harmonics of airload included in procedure
NMASS	Number of tuning masses included in procedure
NMODE	Number of modes included in procedure
NTIME	Number of critical time points in one revolution of blade
q_{ik}	Response of ith mode subject to k/rev harmonic of airload
$\lvert q_{ik} \rvert$	Amplitude of the response of ith mode to k/rev harmonic of airload
S	Amplitude of the blade root vertical shear force, lbf
S_{ik}	Amplitude of the modal shear force corresponding to the ith mode and k/rev harmonic of airload, lbf
S_k	Amplitude of the shear force associated with the k/rev harmonic of airload, lbf
s	Time variation of blade root vertical shear force, lbf
s_{ik}	Time variation of modal shear force corresponding to ith mode and k/rev harmonic of airload, lbf
t	Time, seconds
t_m	Critical time, seconds
v_j	jth design variable
s_{max}	Maximum peak shear in one blade revolution, lbf
X_n	Locations of the tuning masses along blade span, inches
$\beta, \beta_k, \beta_{ik}$	Additional design variables
ξ_i	Damping coefficient
ϕ_k	Phase angle of k/rev harmonic
$\{\phi_i\}$	Eigenvector for ith mode
γ_{ik}	Phase angle
ω_i^2	Eigenvalue equal to the square of the ith natural frequency, rad/s

Ω Angular velocity of blade, rpm or rad/s

ω_{li} Lower bound on frequency, rad/s

ω_{ui} Upper bound on frequency, rad/s

ρ Adjustable tolerance factor (see Eq. (37))

Δv_j Change in jth design variable

Subscripts

i Denotes ith mode

j Denotes jth design variable

k Denotes kth harmonic of airload

Superscript

T Denotes transpose of a matrix

INTRODUCTION

The current trend in engineering design of aircraft and spacecraft is to incorporate critical requirements from all pertinent disciplines analytically in an early phase of the design process to avoid the costly modification of a prototype after a problem has been detected (Ref. 1). Incorporation of vibration requirements in rotorcraft design is one example of this. In helicopter rotor blade and fuselage design, the need to increase ride comfort, stability, and fatigue life of structural components leads to stringent design constraints on vibration levels (Refs. 2-4).

Vibration is transmitted from the blade to the fuselage primarily through a time-dependent shear force at the hub. Historically, frequency placement has been the principal technique for reducing rotor blade vibration (Refs. 5 and 6). Recently, it has been shown that minimization of the hub shear can be achieved through minimization of a modal shaping parameter (MSP) (Refs. 2 and 3). An associated technique, sometimes referred to as "modal shaping" or "modal tailoring", alters the vibration mode shapes of the blades through mass and/or stiffness modification to make them less responsive to the airloads (Refs. 2, 7-9). A number of passive control techniques show promise for overall reduction of structural vibration in rotor blades. For example, pendulum absorbers (Ref. 10), active isolation devices (Ref. 11), additional damping (Refs. 4, 11-12), and vibration absorbers which create anti-resonances (Refs. 13-14) have been demonstrated. Particularly effective is the strategic placement of tuning masses along the blade span to tailor mode shapes (Refs. 2-3, 5). What has been lacking in modal shaping and frequency placement methods is a systematic approach for predicting the best locations for the tuning masses along the blade span.

The purpose of this paper is to develop and demonstrate a method for optimally locating, as well as sizing, tuning masses to reduce vibration using formal mathematical optimization techniques. The design goal is to find the best combination of tuning masses and their locations to minimize blade root vertical shear without a large mass penalty. The method is to formulate and solve an optimization problem in which the tuning masses and their locations are design variables that minimize a combination of blade shear and the added mass with constraints on frequencies to avoid resonance.

The optimization procedure includes a finite-element vibration analysis (Ref. 15) of a rotor blade in combination with a general-purpose optimization code (Ref. 16). An explicit, approximate analysis (Ref. 17) of the blade vibration behavior is used to avoid the high computational cost of repeating the finite-element analysis for every blade modification. Sensitivity derivatives of the structural behavior with respect to the design variables are required in the optimization procedure. The research described herein includes development of the finite-element formulation of the analytical sensitivity derivatives of the MSP and the blade root vertical shear.

Three alternate optimization strategies are developed and demonstrated in the paper. The first is based on minimizing the modal shaping parameter, thus reducing amplitudes of the modal shear for a single mode and single harmonic of the airloading. The second strategy directly reduces the shear amplitudes corresponding to several harmonics for several modes, and the third strategy reduces the total shear as a function of time during a revolution of the blade. Results are shown in which the above strategies are applied to a rotor blade design considering single mode/single harmonic airload, as well as multiple mode/multiple harmonic airload cases.

ROTOR BLADE DYNAMIC ANALYSIS CONSIDERATIONS

Calculation of the natural vibration mode shapes and frequencies, and the steady-state harmonic response are the fundamental analysis steps in the optimization procedure to be described. The purpose of this section of the paper is to outline the analytical basis and modeling conventions for the calculations.

The rotor blade is modeled as a pinned-free beam undergoing lateral vibration normal to the plane of the rotor disk. This "flapwise" motion is in general accompanied by in-plane (edgewise) motion as well as torsion, but these are not included in this work. The beam is assumed to rotate at a constant speed (the rotor speed) about an axis which passes through the pinned end of the beam and is normal to the rotor disk. The effects of blade rotation are included through the centrifugal stiffness terms and differential stiffness terms in the equation of motion (see appendix). An additional term due to the Coriolis acceleration generally occurring in the equations of motion of rotating structures is not necessary in the model used herein. Also, damping is neglected in the calculation of frequencies and mode shapes and although it is often included in response calculations as modal damping, damping is neglected in all calculations herein. Based on the preceding, the governing equation for the finite-element modeled rotor blade is

$$M\ddot{X} + KX = F$$

where M is the mass matrix

K is the stiffness matrix

F is the applied force vector

Solution of the governing equation is described in more detail in the appendix, along with a discussion of how the centrifugal effects are included.

The time-dependent forces acting on the rotor blade are associated with the lift and drag forces generated by the air flow passing through the rotor disk. These loads are spatially distributed along the blade and vary with time sinusoidally at frequencies which are integer multiples (harmonics) of the rotor speed. It is customary in rotorcraft dynamics to use the notation N/rev or N per rev when referring to frequencies or loading at N times the rotor speed. In rotor blade dynamic response, it is generally assumed that the loads are specified in terms of distributions and phases for all appropriate harmonics. For an N-bladed rotor, the most critical frequencies of load and response are $N\Omega$ and $(N \pm 1)\Omega$. Thus the most important harmonics are N and N ± 1.

In the work described in this paper, the blade flapwise response is calculated by modal superposition. An outline of the derivation is given in the appendix, mainly for the purpose of establishing the terminology, but also for completeness. The flapwise modes which have the largest contribution to vertical shear transmitted from the blade to the fuselage are the first and second elastic modes. Therefore these two modes are included in the example problems described in subsequent sections of the paper.

DERIVATION OF PERFORMANCE PARAMETERS AND THEIR SENSITIVITY DERIVATIVES

The degree to which the design is optimized is measured by two performance parameters: the modal shaping parameter (MSP) and the amplitude of the blade root vertical shear S. This section of the paper contains derivations of these performance parameters and their sensitivity derivatives. The roles they play in the optimization will be discussed in a subsequent section of the paper.

Derivation of MSP and Shear

Reference 2 derives an expression for the vertical shear contribution, s_{ik}, from the ith flapwise mode due to the kth harmonic of the airload for a distributed parameter model of a rotor blade. This paper develops its finite-element counterpart. Readers who are not familiar with Reference 2 may find the appendix helpful.

From Equation (11) of Reference 2, the expression for s_{ik} is

$$s_{ik} = q_{ik} \cdot \omega_i^2 \int m\phi_i \, dx \qquad (1)$$

where q_{ik} is the steady state modal response (derived in appendix)

ω_i is the ith natural frequency

ϕ_i is the ith eigenvector

and m is the mass per unit length

For a discrete (finite-element modeled) structure, the analogous expression is

$$s_{ik} = q_{ik} \, \omega_i^2 \{U\}^T [M] \{\phi_i\} \qquad (2)$$

where [M] is the diagonal mass matrix and {U} is a selection vector that extracts the appropriate components from the eigenvector. For example, for modal shaping of the flapwise modes, {U} contains 1.0 in the rows corresponding to the flap degree of freedom and 0.0 elsewhere. Using Equation (A8) from the appendix for the time dependence of q_{ik} and letting

$$a_i = \omega_i^2 \{U\}^T [M] \{\phi_i\} \qquad (3)$$

gives

$$s_{ik} = S_{ik} \sin(k\Omega t + \gamma_{ik}) \qquad (4)$$

where $S_{ik} = a_i |q_{ik}|$ (5)

Ω is the angular velocity of the rotor blade

t is time

and γ_{ik} represents a phase difference between the components of the response. This phase angle accounts for the lag between the modes, as well as the harmonics of the force. For cases in which there is no damping, γ_{ik} reduces to ϕ_k which is the phase angle for the kth harmonic (see appendix for more details of γ_{ik}).

The time variation of the total shear results from summing over the modes and harmonics

$$s(t) = \sum_k \sum_i S_{ik} \sin(k\Omega t + \gamma_{ik}) \qquad (6)$$

Substituting Equation (A9) from the appendix for $|q_{ik}|$ and Equations (3) and (5)

$$S_{ik} = \frac{\{U\}^T [M] \{\phi_i\}}{\tilde{M}_i} \cdot DAF_{ik} \cdot F_{ik} \qquad (7)$$

where for the case of no damping ($\xi = 0$) the dynamic amplification factor DAF_{ik} is

$$DAF_{ik} = \frac{(\omega_i/k\Omega)^2}{[(\omega_i/k\Omega)^2 - 1]} \tag{8}$$

$\bar{M}_i$ is the generalized mass

F_{ik} is the generalized force, (Equation (A10)) written as

$$F_{ik} = A_k\{F_k\}^T\{\phi_i\} \tag{9}$$

A_k is the amplitude of the force and $\{F_k\}$ is the force distribution for the kth harmonic. Using Equations (7)-(9) and rearranging terms leads to the expression

$$S_{ik} = \frac{\{U\}^T[M]\{\phi_i\} \cdot \{F_k\}^T\{\phi_i\}}{\bar{M}_i} \cdot DAF_{ik} \cdot A_k \tag{10}$$

The total contribution from all the modes to the kth harmonic of shear is

$$S_k = \sum_i S_{ik} \tag{11}$$

Following Taylor (Ref. 2), the first term of Equation (10) is identified as the modal shaping parameter (MSP). Thus

$$MSP_{ik} = \frac{\{U\}^T[M]\{\phi_i\} \cdot \{F_k\}^T\{\phi_i\}}{\bar{M}_i} \tag{12}$$

Equation (12) shows that an MSP exists for each mode shape and load case (harmonic). Since the MSP is a function of the mode shape, it is possible to reduce its value by tailoring the mode shape. For example, if the mode shape is made orthogonal to the force distribution, then the value of the MSP is zero. As seen from Equation (10), S_{ik} can be reduced by reducing MSP_{ik} while limiting the size of DAF_{ik}. The size of DAF_{ik} is controlled by placing constraints on the natural frequencies as suggested in Reference 5. Equations (6), (10), (11), and (12) are the basis for the optimization strategies which will be discussed in a later section of the paper.

Derivation of Sensitivity Derivatives of Performance Parameters

Derivative of MSP_{ik} - Beginning with Equation (12) the derivative of the MSP can be calculated as:

$$\bar{M}_i \frac{\partial MSP_{ik}}{\partial v_j} = \left(\{U\}^T[M]\left\{\frac{\partial \phi_i}{\partial v_j}\right\} + \{U\}^T\left[\frac{\partial M}{\partial v_j}\right]\{\phi_i\}\right) \cdot \{F_k\}^T\{\phi_i\} + \{U\}^T[M]\{\phi_i\} \cdot \{F_k\}^T\left\{\frac{\partial \phi_i}{\partial v_j}\right\}$$

$$j = 1,2,\ldots,NDV \tag{13}$$

where NDV is the number of design variables. In Equation (13) $\{\partial\phi_i/\partial v_j\}$ is the derivative of the ith eigenvector with respect to the jth design variable which is calculated analytically by Nelson's method (Ref. 18) and $[\partial M/\partial v_j]$ is the derivative of the mass matrix which is calculated by finite differences. For the design variables used (masses and locations) the finite difference derivatives are exact.

Derivative of S_{ik} - Using Equations (10) and (12) we can write the amplitude of the shear as

$$S_{ik} = MSP_{ik} \cdot DAF_{ik} \cdot A_k \tag{14}$$

and then the derivative is

$$\frac{\partial S_{ik}}{\partial v_j} = \frac{\partial MSP_{ik}}{\partial v_j} \cdot DAF_{ik} \cdot A_k + MSP_{ik} \cdot \frac{\partial DAF_{ik}}{\partial v_j} \cdot A_k \tag{15}$$

where $\frac{\partial MSP_{ik}}{\partial v_j}$ is taken from Equation (13) and the derivative of the dynamic amplification factor (DAF) of Equation (8) is

$$\frac{\partial DAF_{ik}}{\partial v_j} = -\frac{1}{(k\Omega)^2[(\omega_i/k\Omega)^2 - 1]^2} \frac{\partial(\omega_i^2)}{\partial v_j} \tag{16}$$

In Equation (16) ω_i^2 is the ith eigenvalue. The derivative $\frac{\partial \omega_i^2}{\partial v_j}$ can be calculated analytically with the following equation (Ref. 19):

$$\frac{\partial \omega_i^2}{\partial v_j} = \{\phi_i\}^T\left[\frac{\partial [K]}{\partial v_j} - \omega_i^2 \frac{\partial [M]}{\partial v_j}\right]\{\phi_i\} \tag{17}$$

where $\frac{\partial [K]}{\partial v_j}$, the derivative of the stiffness matrix with respect to the jth design variable, is calculated by finite differences.

Equations (13) and (15) are the expressions for the derivatives of the performance parameters which are

used in the sensitivity calculations for the three different optimization strategies.

OPTIMIZATION FORMULATION

Design Goal

The design goal is to find the optimum combination of tuning masses M_n and their locations X_n (Fig. 1) to minimize blade root vertical shear while avoiding an excessive mass penalty. The method is to formulate and solve an optimization problem in which the tuning masses and locations are design variables that minimize the objective function which is a combination of a measure of vertical shear and the added mass. Additionally, constraints are placed on the frequencies to avoid resonance. It is noted that because this optimization formulation involves mass as the objective function and frequencies and harmonic response as constraints, it falls into the general category of optimization problems discussed in Reference 20. In that reference, the complication of a disjoint design space was identified as occurring - the disjointedness being associated with noncontiguous regions of the design space on either side of resonance points. It turns out that in the current formulation, the disjoint design space problem was avoided because in rotor blades, frequency changes due to varying tuning masses tend to be small. Also, even when the disjoint problem occurs it may be dealt with by generating several designs from different starting points - a technique which is generally used when the presence of multiple local minima is suspected.

Three optimization strategies will be described in this section of the paper. In each method, additional design variables (β) are used. They facilitate the trade off between desired performance and excessive mass penalty. A general-purpose constrained optimization program, CONMIN (Ref. 16), is used. CONMIN requires derivatives of the objective function and constraints. All derivatives are obtained analytically as will be shown in this section.

Strategy I

The objective function is

$$f = \left(1 + \sum_k \sum_i \beta_{ik}\right) \sum_{n=1}^{NMASS} M_n \tag{18}$$

where i is an element of the set of included modes (I) and k is an element of the set of included harmonics of airload (K), M_n are the tuning masses, and β_{ik} are the additional design variables which also appear in the constraints defined below:

$$MSP_{ik} \leq \beta_{ik} \qquad \begin{matrix} i \in I \\ k \in K \end{matrix} \tag{19}$$

or in standard dimensionless form:

$$g = MSP_{ik}/\beta_{ik} - 1 \leq 0 \tag{20}$$

These constraints express the requirement that the MSP_{ik} be less than β_{ik}. The convention is that for $g \leq 0$ the constraint is satisfied and violated otherwise. Large values of β_{ik} make the constraints easy to satisfy, but cause a large objective function. Conversely, small values of β_{ik} result in a small objective function, but make the constraints more difficult to satisfy. The optimizer, therefore, will tend toward designs with the lowest possible values of β_{ik} and therefore low values of MSP_{ik}. Additional constraints include upper and lower bounds on the frequencies to avoid resonance

$$\omega_{li}^2 \leq \omega_i^2 \leq \omega_{ui}^2 \tag{21}$$

or

$$g = \omega_i^2/\omega_{ui}^2 - 1 \leq 0$$

and (22)

$$g = 1 - \omega_i^2/\omega_{li}^2 \leq 0$$

The required derivatives of the objective function and constraints are obtained by differentiating Equations (18), (20), and (22). The derivative of the objective function is

$$\frac{\partial f}{\partial v_j} = \begin{cases} 0 & v_j = X_n \\ 1 + \sum_k \sum_i \beta_{ik} & v_j = M_n \\ \sum_{n=1}^{NMASS} M_n & v_j = \beta_{ik} \end{cases} \tag{23}$$

Using the dimensionless form of the constraint function (Eq. (20)), the derivatives of the constraints are expressed as

$$\frac{\partial g}{\partial v_j} = \begin{cases} -MSP_{ik}/\beta_{ik}^2 & v_j = \beta_{ik} \\ \frac{1}{\beta_{ik}} \frac{\partial MSP_{ik}}{\partial v_j} & v_j = X_n \text{ or } M_n \end{cases} \tag{24}$$

where Equation (13) is used for calculating the derivative of MSP_{ik}. The constraints on the frequencies also need to be differentiated. Taking the derivative of Equation (22) gives

$$\frac{\partial g}{\partial v_j} = \begin{cases} 0 & v_j = \beta_{ik} \\ \frac{1}{\omega_{ui}^2} \frac{\partial \omega_i^2}{\partial v_j} \text{ and } -\frac{1}{\omega_{li}^2} \frac{\partial \omega_i^2}{\partial v_j} & v_j = X_n \text{ or } M_n \end{cases} \tag{25}$$

Equation (17) is used for calculating the eigenvalue derivative, $\frac{\partial \omega_i^2}{\partial v_j}$.

Strategy II

In this strategy the constraints are placed on the harmonic amplitudes, S_k (see Eq. (11)). The objective function is

$$f = \left(1 + \sum_k \beta_k\right) \sum_{n=1}^{NMASS} M_n \tag{26}$$

The additional design variables β_k play a role similar to β_{ik} in the first strategy. Here the constraints are written as

$$S_k \leq \beta_k \qquad k \in K \tag{27}$$

or

$$g = S_k/\beta_k - 1 \leq 0 \tag{28}$$

This strategy also employs upper and lower bound constraints on the frequencies (Eqs. (21) and (22)).

Similar to strategy I, the derivative of the objective function is obtained by differentiating Equation (26).

$$\frac{\partial f}{\partial v_j} = \begin{cases} 0 & v_j = X_n \\ 1 + \sum_k \beta_k & v_j = M_n \\ \sum_{n=1}^{NMASS} M_n & v_j = \beta_k \end{cases} \tag{29}$$

Differentiating Equation (28) gives the derivatives of the constraints

$$\frac{\partial g}{\partial v_j} = \begin{cases} -S_k/\beta_k^2 & v_j = \beta_k \\ \dfrac{1}{\beta_k}\dfrac{\partial S_k}{\partial v_j} & v_j = X_n \text{ or } M_n \end{cases} \tag{30}$$

where $\dfrac{\partial S_k}{\partial v_j} = \sum_i \dfrac{\partial S_{ik}}{\partial v_j}$, and $\dfrac{\partial S_{ik}}{\partial v_j}$ is given in Equation (15). Equations (25) and (17) give the derivatives of the frequency constraints.

Strategy III

In this formulation, the shear as a function of time is minimized by constraining all the peak values which occur during a revolution of the blade. These are called critical point constraints (Ref. 21). The objective function is

$$f = [1 + \beta] \sum_{n=1}^{NMASS} M_n \tag{31}$$

and the constraints are

$$s(t_m) \leq \beta \qquad m = 1,2,\ldots,NTIME \tag{32}$$

or

$$g = s(t_m)/\beta - 1 \leq 0 \tag{33}$$

which require that the values of the shear at each time t_m be less than the value of β; and again β is minimized because of its role in the objective function. As shown in Equation (6), $s(t_m)$ is the shear at time t_m where t_m represents a time at which a peak occurs in $s(t)$.

The peak values are identified as follows: A value of NTIME is specified corresponding to the maximum number of peaks in the function $s(t)$ during a revolution of the blade. The peak values are identified by examining the shear as a function of time (Ref. 21). The constraints are placed on these NTIME values of shear to force the peaks to be as small as possible. This procedure does not require that the locations of the peaks be constant throughout the optimization process since the search for the peaks occurs each time the analysis is performed for a new set of design variables. Additional constraints are again placed on the upper and lower values of the frequencies (Eqs. (21) and (22)). Again the objective function for strategy III yields a similar derivative as in the two previous cases

$$\frac{\partial f}{\partial v_j} = \begin{cases} \sum_{n=1}^{NMASS} M_n & v_j = \beta \\ 0 & v_j = X_n \\ 1 + \beta & v_j = M_n \end{cases} \tag{34}$$

Differentiating Equation (33) with respect to the design variables gives*

$$\frac{\partial g}{\partial v_j} = \begin{cases} -s(t_m)/\beta^2 & v_j = \beta \\ \dfrac{1}{\beta}\dfrac{\partial s(t_m)}{\partial v_j} & v_j = X_n \text{ or } M_n \end{cases} \tag{35}$$

where $s(t_m)$ is obtained from Equation (6) and $m = 1,2,\ldots,NTIME$. The derivative of the shear $\dfrac{\partial s(t_m)}{\partial v_j}$ at time t_m is

$$\frac{\partial s(t_m)}{\partial v_j} = \sum_k \sum_i \frac{\partial S_{ik}}{\partial v_j} \sin(k\Omega t_m + \phi_k) \tag{36}$$

where the derivative $\dfrac{\partial S_{ik}}{\partial v_j}$ is given by Equation (15).

*The critical point t_m is also a function of the design variables; however, as pointed out in Reference 21 this has no effect on the derivative in Equation (35).

KS-Function

It can be seen from the optimization formulations that as we begin to consider the contributions of larger numbers of modes and load cases to the shear, or as the number of critical points in strategy III increases, the number of constraints will become large. This can cause slower convergence of the optimization process. An envelope constraint function, denoted the Kreisselmeier-Steinhauser (KS) function (Ref. 22), is used to substitute a single constraint function for a large number of constraints. The KS-function is defined as

$$KS = \frac{1}{\rho} \ln\left(\sum_{i=1}^{NCON} e^{\rho g_i}\right) \tag{37}$$

where the g_i are the actual constraints, NCON is the number of constraints, and ρ controls the distance between the KS-function and the actual constraint boundary (Fig. 2). For small values of ρ, the KS-function is very smooth and also a very conservative estimate of the constraint violations. As ρ increases, the KS-function moves closer to the discontinuous function, $\max_i (g_i)$. Typically, the initial value of ρ is small and is increased as convergence is approached.

The optimizer requires the derivative of the KS-function. Taking the derivative of Equation (37) gives

$$\frac{\partial KS}{\partial v_j} = \frac{\sum_{i=1}^{NCON} e^{\rho g_i} \frac{\partial g_i}{\partial v_j}}{\sum_{i=1}^{NCON} e^{\rho g_i}} \tag{38}$$

where $\frac{\partial g_i}{\partial v_j}$ are derivatives of the constraints.

OPTIMIZATION PROCEDURE

The sequence of operations in the optimization procedure is illustrated in Figure 3. The overall procedure consists of two nested loops. Each pass through the outer loop is referred to as a cycle which involves a full analysis and a sensitivity calculation. The first step is to generate the finite-element structural model of the beam, excluding the values of tuning masses. The design variables (masses and locations) are used to allocate the masses to the appropriate grid points of the model. Specifically, the masses M_n are divided between the two grid points adjacent to each X_n by prorating according to the distance from each. Next, the masses are inserted into the model, the vibration analysis is performed, and the MSP_{ik} and shear amplitudes S_{ik} are calculated for NMODE number of modes responding to NHARM number of harmonics. The sensitivity analysis includes calculating the vibration mode shape derivatives by Nelson's method and then calculating the derivatives of the objective function and constraints using Equations (23)-(25) for strategy I, Equations (25) and (29)-(30) for strategy II, and Equations (25) and (34)-(36) for strategy III. The inner loop consists of the optimization program, CONMIN (Ref. 16) and an approximate analysis for calculating the objective function and the constraints (see Ref. 17). The approximate equations are

$$f = f_o + \sum_{j=1}^{NDV} \frac{\partial f}{\partial v_j} \Delta v_j \tag{39}$$

$$g = g_o + \sum_{j=1}^{NDV} \frac{\partial g}{\partial v_j} \Delta v_j \tag{40}$$

These equations give the change in the objective function from f_o to f and the change in a constraint from g_o to g corresponding to a change in design variable Δv_j. To assure that the linear approximation in Equations (39) and (40) are valid, the size of Δv_j is limited to 10 percent of v_j. Use of these approximations saves computational time and effort in the inner loop where many evaluations of the objective function and constraints are required. Development of these and other techniques and demonstration of their benefits are described in Reference 23. It was observed that the KS-function of the linear approximation to g was a very accurate approximation to the KS-function of the exact g. Once the inner loop iterations have converged the next cycle of the outer loop begins, using the current design variables as the new values of the lumped masses and their locations. These masses are then inserted into the structural model and the process continues until convergence of the outer loop is achieved.

EXAMPLE PROBLEM

The example problem is a beam representation of an articulated rotor blade developed in Reference 5 and shown in Figure 4. The beam is 193 inches long with a hinged end condition and is modeled by 10 finite elements of equal length. The model contains both structural mass and lumped (non-structural) masses. The beam has a box cross section as shown in Figure 4b and the material properties and cross-sectional dimensions are summarized in table 1. Three lumped masses are to be placed along the length of the beam. The values of the masses and their locations are the design variables and their initial values, shown in table 1, are from the blade in Reference 5.

Figure 5 shows the distributions (from Ref. 2) and phase angles (from Ref. 24) of the airloads used. They are input as tabulated values of distributed forces (i.e., force per unit length) into the finite-element analysis (Ref. 15). The forces $\{F_k\}^T$ needed in Equation (9) are calculated as consistent nodal forces for the finite-element model. These airloads represent the 3, 4, and 5 per rev lifting airloads that are typical of a four-bladed articulated rotor system. These harmonics were chosen since they are the prime contributors to the vibration of a four-bladed rotor system. In this work, the first and second elastic flapping modes are included since they are prime contributors to the vertical vibration transmitted by the rotor blades to the fuselage.

RESULTS AND DISCUSSION

The following sections discuss results obtained for each of the three optimization strategies applied to the example problem. The test cases include (1) a single mode responding to a single harmonic of the airload; (2) two modes responding to a single harmonic of airload; and (3) two modes responding to three harmonics of the airload.

Results for Strategy I

Figures 6a and 6b show the initial and final designs for the first test case using strategy I for minimizing S_{14}, the shear for the first elastic flapping mode and the 4/rev airload by proper placement of three tuning masses. The 4/rev airload is concentrated at the tip of the blade and in order to shape the mode to be insensitive to the airload all three tuning masses were moved to the tip of the blade. Figure 6c shows a sketch of the mode shape before and after optimization. It is this change in the mode shape that reduces the value of the MSP_{14} 99 percent and the corresponding shear S_{14} by a similar amount. Table 2 summarizes the initial and final designs. It is noted that the large change in MSP and shear is accompanied by an almost zero change in frequency.

This method proved to be very useful when working on the response of one mode corresponding to one airload; however, when this method was applied to more than one mode it was not always effective. The method did reduce the values of the MSP's as required, but low values of the MSP's did not necessarily give low values for the shear, S_k. The reason for this is that the various MSP's (and, therefore, the corresponding contributions to the shear, S_{ik}) may have different signs. When these shear contributions are added together (see Eq. (11)), small values for the individual contributions S_{ik} do not always minimize the shear S_k unless the necessary cancelling of equal and opposite terms occurs.

Results for Strategy II

In strategy II, the method is to reduce the values of the shear contributions, S_{ik} summed over the modes (see Eq. (11)). This eliminates the problem in strategy I since constraints placed on the sums of the modal shears encourage the desirable cancellation effects. The first step in demonstrating this method was to validate it for the 1 mode/1 load case. The design for strategy II is essentially identical to that of Figure 6 and table 2 gives the initial and final designs of the blade. The next step was to apply this strategy to a 2 mode/1 load case. The response of the first and second elastic flapping modes corresponding to the 4/rev airload is minimized. Table 3 summarizes the initial and final designs. The initial shear S_4 including both modes is -34.68 lbf which is reduced by the optimization process to -.01 lbf with an accompanying decrease in the added mass.

Inspection of the initial and final values of the MSP's (table 3) shows that the magnitudes of the MSP's became larger. This helps to explain the lack of success of strategy I for this problem. In fact, the modal shears S_{14} and S_{24} are equal and opposite thus combining together to produce a near zero value of total shear. Figures 7a and 7b show the initial and final masses and their locations and Figure 7c shows the change in the shapes of the first and second elastic flapwise modes.

Strategy II was next applied to a case of two modes responding to the 3, 4, and 5 per rev harmonics of airloading (see Fig. 5). Table 4 shows the initial and final results where the amplitudes of the shears, due to the two flapwise modes, have been reduced significantly with only a 9 lbm increase in tuning mass. For example, S_5, the shear force associated with the 5/rev harmonic, was reduced from -39.48 lbf to -.162 lbf. Figure 8 gives a time history of the shear during one revolution of the blade before and after optimization. It is clear from the figure that reducing the amplitudes of the harmonic shears results in a large reduction of the total shear throughout a revolution of the blade.

Results for Strategy III

The third strategy was applied to the previous test case of two modes responding to three harmonics. Figure 9 shows graphs of the shear s(t) plotted as a function of time and azimuth for a revolution of the blade for the initial and final designs. The peaks on the initial curve have been reduced dramatically. For example, the maximum peak s_{max} for the initial design is -78.00 lbf and for the final design the maximum peak is -.576 lbf. The extreme right column in table 4 gives details of the final designs from strategy III and indicates a large payoff for a relatively small increase in added mass.

Comparison of Strategies II and III

As seen from table 4, strategy III gave a design comparable to strategy II. In both cases, there was a significant reduction in the total shear. Results from strategies II and III are compared in table 5, in terms of the peak values of s(t) at the critical points. The final results were very close with strategy III producing slightly lower values for some of the peaks and strategy II producing lower values of others. Overall, strategy III was slightly better in minimizing the peak shear. Figure 10 shows the shears plotted as functions of time from each strategy. Strategy III was a somewhat more complicated approach than strategy II and was more cumbersome to implement. However, the greater degree of rigor in strategy III makes the slightly greater effort worth the investment.

CONCLUDING REMARKS

This paper described methods for systematically locating, as well as sizing, tuning masses to reduce vibration in helicopter rotor blades using formal mathematical optimization techniques. The problem was to find the optimum combination of tuning masses and their locations to reduce vertical shear without a large mass penalty. The methods embodied optimization procedures in which tuning masses and their locations were design variables whose values minimize a combination of shear and added mass. The finite-element

structural analysis of the blade and the optimization formulations required the development of discretized expressions for two performance parameters: the modal shaping parameter, and the amplitude of the blade root vertical shear. Matrix expressions for both quantities and their sensitivity derivatives were derived in this paper. The mechanism in the optimization for reducing the vertical blade shear was through "modal shaping" by placing the tuning masses at strategic locations along the blade.

Three optimization strategies were developed: the first was based on minimizing the modal shaping parameter, thus indirectly reducing the amplitudes of the modal shear for each harmonic; the second reduced the shear amplitudes directly; and the third reduced the total shear as a function of time during a revolution of the blade.

Strategy I worked well for reducing the shear for one mode responding to one harmonic of the load, but was ineffective for multiple modes. This was due to inability of the method to take advantage of sign differences between the contributions for different modes and harmonics. Strategy II worked extremely well for the 1 mode/1 load case, as well as multiple mode/multiple loads. Strategy III gave excellent results; that is, the peak shear was reduced significantly without a large mass penalty. Strategies II and III gave esentially the same results for a 2 mode/3 load case. Strategy II is slightly easier to implement but the fact that strategy III is a more rigorous approach makes it a preferred choice overall.

APPENDIX

DERIVATION OF GENERAL FORM OF STEADY-STATE RESPONSE OF A HELICOPTER ROTOR BLADE

The purpose of this appendix is to develop the general form of the steady-state modal response q_{ik} for the ith mode and kth harmonic of loading. This derivation is based on that of Reference 2 and is included here to establish the notational conventions used in the main body of the paper in the expressions for the modal shaping parameter (MSP) and blade root vertical shear (S).

The governing matrix equation for vibration response of a finite-element modeled structure is

$$M\ddot{X} + C\dot{X} + KX = F \tag{A1}$$

where M is the mass matrix

C is the damping matrix

K is the stiffness matrix

X is the vector of displacements and rotations

F is the applied force vector

The stiffness matrix K for a rotor blade has the form

$$K = K_E + K_C + K_D \tag{A2}$$

where K_E is the linear elastic stiffness matrix

K_C is a centrifugal stiffness matrix which contains products of masses and angular velocity

K_D is the differential stiffness matrix and contains stresses associated with extension of the beam due to centrifugal forces

Details of the derivations and explicit forms for K_C and K_D may be found in References 25 and 26.

Express the response vector X as a modal expansion such that

$$X = \sum_{i=1}^{NMODE} \phi_i q_i \tag{A3}$$

where ϕ_i is the ith vibration mode of the structure

q_i is the generalized response vector

The modes are normalized such that

$$\phi_i^T M \phi_i = \bar{M}_i \tag{A4}$$

Equation (A4) is the usual definition of $\bar{M}_i$ as the generalized mass associated with the ith mode. Combining Equations (A1), (A3), (A4) gives

$$\ddot{q}_i + 2\xi_i\omega_i\dot{q}_i + \omega_i^2 q_i = \frac{1}{\bar{M}_i} F_i \tag{A5}$$

where ω_i is the natural frequency of the ith mode

F_i is the generalized force for ith mode

ξ_i is modal damping coefficient (see Ref. 27)

Equation (A5) is identical to Equation (1) of Taylor (Ref. 2). The generalized force vector F_i is a superposition of contributions from all harmonics.

$$F_i = \sum_{k=0}^{\infty} F_{ikc} \cos k\Omega t + \sum_{k=1}^{\infty} F_{iks} \sin k\Omega t \tag{A6}$$

From Equation (A5) and (A6) it follows that the steady state modal response amplitudes q_i are of the form

$$q_i = \sum_{k=0}^{\infty} q_{ikc} \cos k\Omega t + \sum_{k=1}^{\infty} q_{iks} \sin k\Omega t \tag{A7}$$

$$= \sum_{k=0}^{\infty} |q_{ik}| \sin(k\Omega t + \gamma_{ik}) \tag{A8}$$

The quantity $|q_{ik}|$ is the amplitude of the response. The defining equation for $|q_{ik}|$ is

$$|q_{ik}| = \frac{F_{ik}}{\bar{M}_i(k\Omega)^2\left\{\left[\left(\frac{\omega_i}{k\Omega}\right)^2 - 1\right]^2 + \left(\frac{2\xi_i\omega_i}{k\Omega}\right)^2\right\}^{1/2}} \quad (A9)$$

where

$$F_{ik} = [F_{iks}^2 + F_{ikc}^2]^{1/2}$$

$$\gamma_{ik} = \psi_{ik} + \phi_k \quad (A10)$$

where

$$\psi_{ik} = \tan^{-1}\left[\frac{2\xi_i\omega_i/k\Omega}{\left(\frac{\omega_i}{k\Omega}\right)^2 - 1}\right] \quad (A11)$$

Equation (A10) along with Equation (A11) show that the phase angle γ_{ik} is composed of the sum of two contributions. The first ψ_{ik} is the usual phase due to damping of the ith mode and the second ϕ_k is due to the phase lag in the kth harmonic of load.

REFERENCES

1. Sobieszczanski-Sobieski, J., "Structural Optimization: Challenges and Opportunities," Paper presented at International Conference on Modern Vehicle Design Analysis (London, England), June 1983.

2. Taylor, R. B., "Helicopter Vibration Reduction by Rotor Blade Modal Shaping," presented at the 38th Annual Forum of the American Helicopter Society, Anaheim, California, May 1982.

3. Taylor, R. B., "Helicopter Rotor Blade Design for Minimum Vibration," NASA CR-3825, 1984.

4. Blackwell, R. H., "Blade Design for Reduced Helicopter Vibration," Journal of the American Helicopter Society, 28, No. 3, July 1983.

5. Peters, D. A., Ko, T., Korn, A., and Rossow, M. P., "Design of Helicopter Rotor Blades for Desired Placement of Natural Frequencies," 39th Annual Forum of the American Helicopter Society, May 1983.

6. Friedmann, P. P., "Application of Modern Structural Optimization to Vibration Reduction in Rotorcraft," NASA CP-2327, Part 2, 553-566, September 1984.

7. Davis, M. W., "Optimization of Helicopter Rotor Blade Design for Minimum Vibration," NASA CP-2327, Part 2, 609-625, September 1984.

8. McCarty, J. L., and Brooks, G. W., "A Dynamic Model Study of the Effect of Added Weight and Other Structural Variations on the Blade Bending Strains of an Experimental Two-Blade Jet-Driven Helicopter in Hovering and Forward Flight," NACA TN-3367, May 1955.

9. Hirsh, H., Hutton, R. E., and Rasamoff, A., "Effect of Spanwise and Chordwise Mass Distribution on Rotor Blade Cyclic Stresses," Journal of the American Helicopter Society, 1, No. 2, 37-45, April 1956.

10. Hamouda, M. H., and Pierce, G. A., "Helicopter Vibration Suppression Using Simple Pendulum Absorbers on the Rotor Blade," Presented at the American Helicopter Society Northeast Region National Specialists' Meeting on Helicopter Vibration, Hartford, Connecticut, November 1981.

11. Reichert, G., "Helicopter Vibration Control - A Survey," Vertica 5, 1-20, 1981.

12. Rogers, L., "Damping as a Design Parameter," Mechanical Engineering, 108, No. 1, January 1986.

13. Wang, B. P., Kitis, L., Pilkey, W. D., and Palazzolo, A., "Synthesis of Dynamic Vibration Absorbers," Journal of Vibration, Acoustics, Stress, and Reliability in Design 107/161, April 1985.

14. Kitis, L., Pilkey, W. D., and Wang, B. P., "Optimal Frequency Response Shaping by Appendant Structures," Journal of Sound and Vibration, 95 (2), 161-175, 1984.

15. Whetstone, W. D., "Engineering Analysis Language Reference Manual - EISI-EAL System Level, 2091," Engineering Information Systems, Inc. EISI-EAL, July 1983.

16. Vanderplaats, G. N., "CONMIN - A Fortran Program for Constrained Function Minimization - User's Manual," NASA TM X-62282, 1973.

17. Walsh, J. L., "Application of Mathematical Optimization Procedures to a Structural Model of a Large Finite-Element Wing," NASA TM-87597, January 1986.

18. Nelson, R. B., "Simplified Calculation of Eigenvector Derivatives," AIAA Journal 14, No. 9, 1201-1205, September 1976.

19. Fox, R. L., and Kapoor, M. P., "Rate of Change of Eigenvalues and Eigenvectors," AIAA Journal, Vol. 6, December 1968, pp. 2426-2429.

20. Mills-Curran, W. C., and Schmit, L. A., "Structural Optimization With Dynamic Behavior Constraints," AIAA Journal, Vol. 23, January 1985, pp. 132-138.

21. Haftka, R. T., and Kamat, M. P., Elements of Structural Optimization," Martinus Nijhoff Publishers, Dordrecht, Netherlands, 1985.

22. Kreisselmeier, G., and Steinhauser, R., "Systematic Control Design by Optimizing a Vector Performance Index," Proceedings of IFAC Symposium on Computer Aided Design of Control Systems, Zurich, Switzerland, 1979, pp. 113-117.

23. Schmit, L. A., and Farshi, B., "Some Approximation Concepts for Structural Synthesis," AIAA Journal, 12, No. 5, 692-699, 1974.

24. Hooper, W. E., "The Vibratory Airloading of Helicopter Rotors," Vertica, Vol. 8, No. 2, 1984, pp. 73-92.

25. Laurenson, R. M., "Modal Analysis of Rotating Flexible Structures," AIAA Journal, Vol. 14, No. 10, October 1976, pp. 1444-1450.

26. Patel, J. S., and Seltzer, S. M., "NASTRAN: User's Experiences," NASA TMX-2378, September 1971.

27. Hurty, W. C., and Rubinstein, M. F., "Dynamics of Structures," Prentice-Hall, Englewood Cliffs, New Jersey, 1964.

Table 1. Details of finite-element model of rotor blade.

(a) Material properties and cross-sectional dimensions (see Figure 4)

Element No.	E (psi)	ρ (lb/in^3)	b (in)	h (in)	t (in)	d (in)
1	0.490×10^7	.07	3.75	2.50	.80	.10
2-10	0.585×10^7	.07	3.75	2.50	.80	.10

(b) Initial values of design variables (see Figure 1)

X_1 (in)	X_2 (in)	X_3 (in)	M_1 (lbm)	M_2 (lbm)	M_3 (lbm)
135.10	154.40	173.70	5.21	6.55	6.60

(c) Blade characteristics

Length (in)	Structural mass (lbm)	Nonstructural mass (lbm)	Ω (rpm)
193	87.82	122.93	425

Table 2. Initial and final designs using strategies I and II for 1 mode/1 load problem. (First elastic flapwise mode at 4/rev)

	Initial	Final	
		Strategy I	Strategy II
X_1 (in)	135.10	193.00	193.00
X_2 (in)	154.40	193.00	193.00
X_3 (in)	173.70	193.00	193.00
M_1 (lbm)	5.21	6.30	6.70
M_2 (lbm)	6.55	10.53	10.33
M_3 (lbm)	6.60	10.60	10.40
M_{TOT} (lbm)	18.36	27.43	27.43
MSP_{14}	-11.75	-0.008	-0.010
S_{14} (lbf)	-58.50	-0.040	-0.051
ω_1 (per rev)	2.69	2.70	2.70

Table 3. Initial and final designs using strategy II for 2 mode/1 load problem. (First and second elastic flapwise modes at 4/rev)

	Initial	Final
X_1 (in)	135.10	135.02
X_2 (in)	154.40	146.38
X_3 (in)	173.70	157.72
M_1 (lbm)	5.21	7.15
M_2 (lbm)	6.55	5.24
M_3 (lbm)	6.60	0.97
M_{TOT} (lbm)	18.36	13.36
S_4 (lbf)	-34.68	-0.01
S_{14} (lbf)	-58.50	-66.91
S_{24} (lbf)	23.82	66.90
MSP_{14}	-11.75	-14.61
MSP_{24}	1.03	2.24
ω_1 (per rev)	2.69	2.63
ω_2 (per rev)	4.65	4.47

Table 4. Initial and final designs using strategies II and III for 2 mode/3 load problem. (First and second elastic flapwise modes at 3, 4, and 5 per rev)

	Initial	Final	
		Strategy II	Strategy III
X_1 (in)	135.10	150.95	152.81
X_2 (in)	154.40	154.44	154.27
X_3 (in)	173.70	154.40	154.42
M_1 (lbm)	5.21	4.28	7.93
M_2 (lbm)	6.55	12.40	9.66
M_3 (lbm)	6.60	10.13	9.26
M_{TOT} (lbm)	18.36	26.81	26.85
S_3 (lbf)	-7.98	-0.36	-
S_4 (lbf)	-34.68	0.30	-
S_5 (lbf)	-39.48	-0.16	-
s_{max} (lbf)	-78.00	-	-0.58
ω_1 (per rev)	2.69	2.81	2.81
ω_2 (per rev)	4.65	4.72	4.72

Table 5. Comparison of peak values of shear during one revolution of the blade using strategies II and III.

Strategy II		Strategy III	
$s(t_m)$ (lbf)	t_m(s)	$s(t_m)$ (lbf)	t_m(s)
-.348	.009	.330	.000
.198	.024	-.186	.014
.162	.044	.234	.042
-.528	.059	-.390	.059
.756	.075	.510	.075
-.768	.092	-.576	.090
-.588	.107	.570	.107
-.402	.121	-.504	.123
.354	.136	.366	.138
.132	.141	-	-

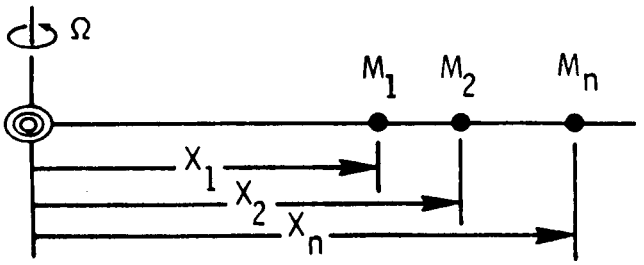

Figure 1. Problem definition: selection of optimum locations for tuning masses

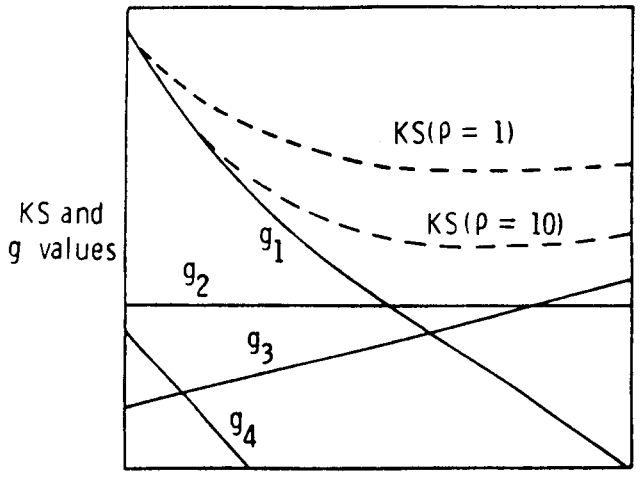

Figure 2. Kreisselmeier-Steinhauser (KS) function

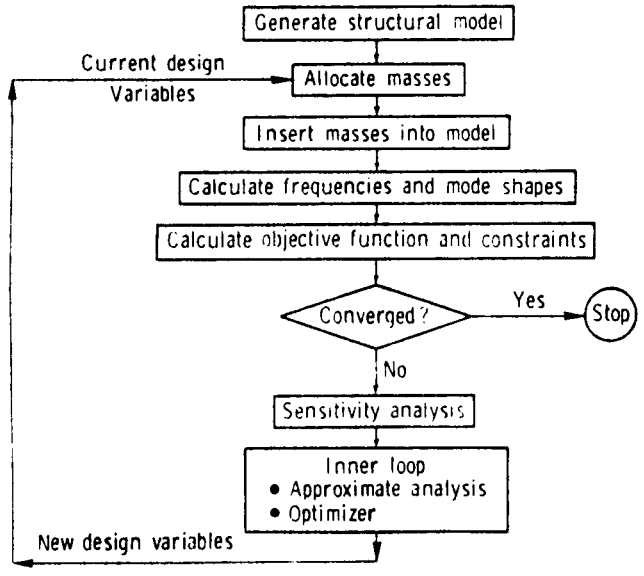

Figure 3. Flow chart for optimization procedure

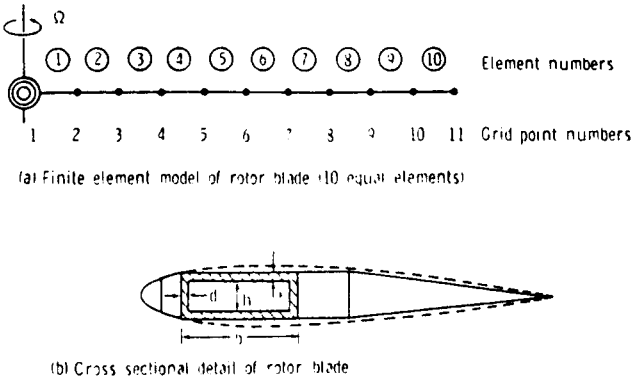

Figure 4. Test problem

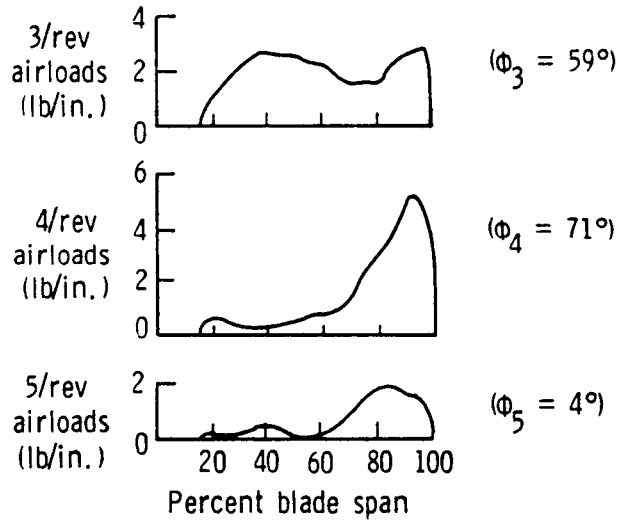

Figure 5. Amplitude distributions and phase angles of airloads

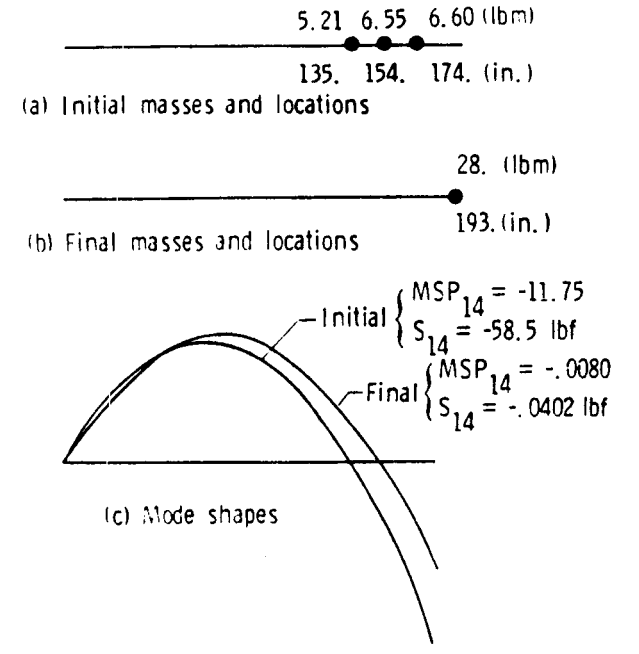

Figure 6. Initial and final designs for 1 mode/ 1 load case using strategy I

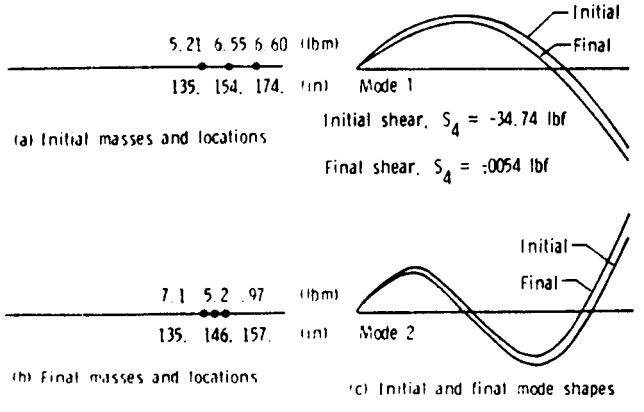

Figure 7. Initial and final designs for 2 mode/ 1 load case using strategy II

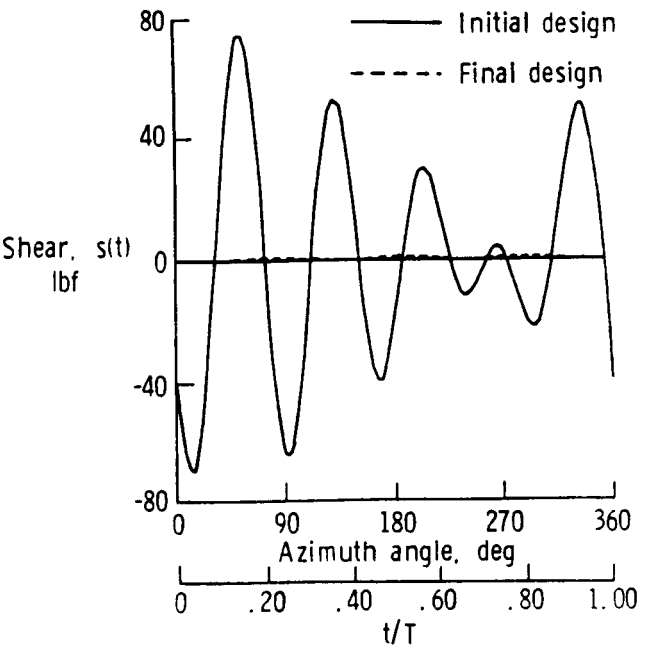

Figure 8. Time history of blade vertical root shear during one revolution. Initial and final designs for 2 mode/3 load case using strategy II

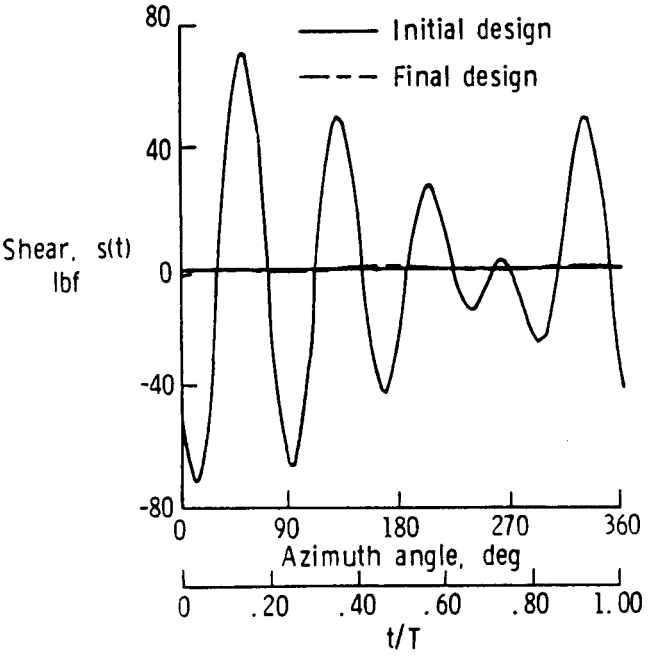

Figure 9. Time history of blade vertical root shear during one revolution. Initial and final designs for 2 mode/3 load case using strategy III

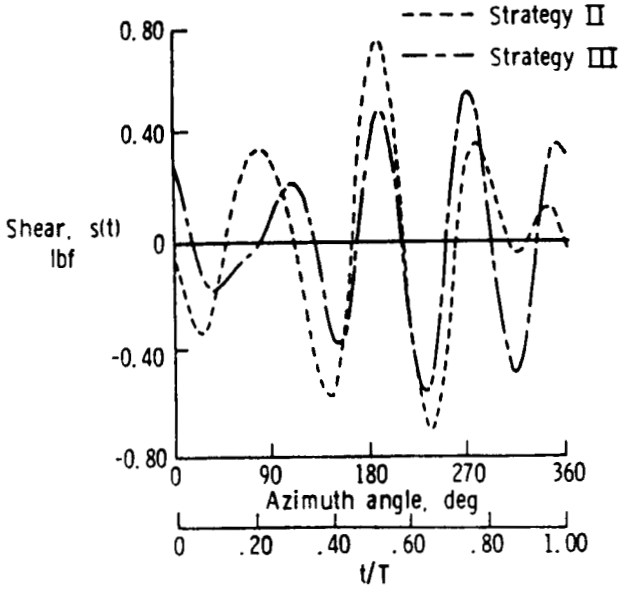

Figure 10. Comparison of final designs from strategies II and III for 2 mode/ 3 load case

NASA National Aeronautics and Space Administration

Report Documentation Page

1. Report No.	2. Government Accession No.	3. Recipient's Catalog No.
NASA TM-100562 AVSCOM TM 88-B-003		

4. Title and Subtitle	5. Report Date
Optimal Placement of Tuning Masses for Vibration Reduction	March 1988
	6. Performing Organization Code

7. Author(s)	8. Performing Organization Report No.
Jocelyn I. Pritchard and Howard M. Adelman	10. Work Unit No. 505-63-51-10

9. Performing Organization Name and Address	11. Contract or Grant No.
NASA Langley Research Center, Hampton, VA 23665 and Aerostructures Directorate, USAARTA-AVSCOM, Hampton, VA 23665	13. Type of Report and Period Covered: Technical Memorandum
12. Sponsoring Agency Name and Address: National Aeronautics and Space Administration, Washington, DC 20546 and U.S. Army Aviation Systems Command, St. Louis, MO 63120-1798	14. Sponsoring Agency Code

15. Supplementary Notes

Jocelyn I. Pritchard, Aerostructures Directorate, USAARTA-AVSCOM, Langley Research Center, Hampton, VA. Howard M. Adelman, Langley Research Center, Hampton, VA. Presented at the 29th AIAA/ASME/ASCE/AHS/ASC Structures, Structural Dynamics and Materials Conference, April 18-20, 1988, Williamsburg, Virginia.

16. Abstract The paper describes methods for reducing vibration in helicopter rotor blades by determining optimum sizes and locations of tuning masses through formal mathematical optimization techniques. An optimization procedure is developed which employs the tuning masses and corresponding locations as design variables which are systematically changed to achieve low values of shear without a large mass penalty. The finite-element structural analysis of the blade and the optimization formulation require development of discretized expressions for two performance parameters: modal shaping parameter and modal shear amplitude. Matrix expressions for both quantities and their sensitivity derivatives are derived. Three optimization strategies are developed and tested. The first is based on minimizing the modal shaping parameter which indirectly reduces the modal shear amplitudes corresponding to each harmonic of airload. The second strategy reduces these amplitudes directly, and the third strategy reduces the shear as a function of time during a revolution of the blade. The first strategy works well for reducing the shear for one mode responding to a single harmonic of the airload, but has been found in some cases to be ineffective for more than one mode. The second and third strategies give similar results and show excellent reduction of the shear with a low mass penalty.

17. Key Words (Suggested by Author(s))	18. Distribution Statement
Modal shaping Optimization Rotor blade vibrations Structural dynamics Mass Placement	Unclassified - Unlimited Subject Category 39

19. Security Classif. (of this report)	20. Security Classif. (of this page)	21. No. of pages	22. Price
Unclassified	Unclassified	15	A02